The Journal of Experimental Biology 211, 921-934
Published by The Company of Biologists 2008
doi:10.1242/jeb.014175

Active sensing in a mormyrid fish: electric images and peripheral modifications of the signal carrier give evidence of dual foveation

Roland Pusch[1], Gerhard von der Emde[1], Michael Hollmann[1], Joao Bacelo[2], Sabine Nöbel[1], Kirsty Grant[2] and Jacob Engelmann[1,*]

[1]University of Bonn, Institute of Zoology, Department Neuroethology/Sensory Ecology, Endenicher Allee 11-13, 43115 Bonn, Germany and [2]UNIC, CNRS, 1 Avenue de la Terrasse, 91190 Gif-sur-Yvette, France

*Author for correspondence (e-mail: jacob.engelmann@uni-bonn.de)

Accepted 11 December 2007

SUMMARY

Weakly electric fish generate electric fields with an electric organ and perceive them with cutaneous electroreceptors. During active electrolocation, nearby objects are detected by the distortions they cause in the electric field. The electrical properties of objects, their form and their distance, can be analysed and distinguished. Here we focus on *Gnathonemus petersii* (Günther 1862), an African fish of the family Mormyridae with a characteristic chin appendix, the Schnauzenorgan. Behavioural and anatomical results suggest that the mobile Schnauzenorgan and the nasal region serve special functions in electroreception, and can therefore be considered as electric foveae. We investigated passive pre-receptor mechanisms that shape and enhance the signal carrier. These mechanisms allow the fish to focus the electric field at the tip of its Schnauzenorgan where the density of electroreceptors is highest (tip-effect). Currents are funnelled by the open mouth (funnelling-effect), which leads to a homogenous voltage distribution in the nasal region. Field vectors at the trunk, the nasal region and the Schnauzenorgan are collimated but differ in the angle at which they are directed onto the sensory surface. To investigate the role of those pre-receptor effects on electrolocation, we recorded electric images of objects at the foveal regions. Furthermore, we used a behavioural response (novelty response) to assess the sensitivity of different skin areas to electrolocation stimuli and determined the receptor densities of these regions. Our results imply that both regions – the Schnauzenorgan and the nasal region – can be termed electric fovea but they serve separate functions during active electrolocation.

Key words: pre-receptor mechanism, active electrolocation, fovea, electric image, shape recognition, electric organ discharge, Mormyridae, *Gnathonemus petersii*.

INTRODUCTION

The electric sense of mormyrid weakly electric fish is generally regarded as an adaptation to a life under conditions not favourable for visual orientation, i.e. a nocturnal life in dark and sometimes turbid waters. Although recent experiments show that the visual system is not as bad as expected in terms of resolution and sensitivity (Ciali et al., 1997; Wagner, 2007), electroreception seems to be the dominant sense for orientation and communication in these animals.

Weakly electric fish explore their environment by the aid of active electrolocation. They generate electric fields and analyze the distortions within the field caused by nearby objects. For object analysis, it is the information contained in the pattern of the voltage changes projected onto the electroreceptive skin areas (electric image) (Caputi and Budelli, 1995) that is relevant for the animals.

Although considerable data exist about the behavioural use of active electrolocation (Lissmann and Machin, 1958; von der Emde, 2006), relatively little attention has been given to the actual physics of the stimuli that the animals experience (Castelló et al., 2000). To further the knowledge of the physical parameters that govern the extraction of environmental information by mormyrids, we were interested in a better description of the signal carrier, i.e. the animal's electric organ discharge (EOD) and the electric field associated with it.

The electrosensory system of *Gnathonemus petersii* is composed of three classes of electroreceptor organs, but of these, the mormyromasts seem to be used in particular for active electrolocation. Mormyromasts are distributed over a large part of the body surface, although with considerable variations in receptor density (Harder, 1968). Because the receptors are located and distributed in the skin, the analysis of electric images of the animal's environment must take into account several factors. A three-dimensional world is projected onto a two-dimensional sensory surface in the skin. In addition, the system lacks a focussing mechanism, hence electric images of objects are always blurred and the amount of blur depends on the object's distance and shape. The curvature of the sensory surface of the head and the trunk, on to which the images are projected, poses additional problems. We speculate that these differences in the way in which the electric world is projected on different regions of the body will have an influence on behavioural strategies employed by the fish and/or on the algorithms used in image analysis during active electrolocation.

In other sensory systems passive mechanisms (pre-receptor mechanisms) are known to enhance relevant sensory signals. In vision, the passive properties of the lens can be regarded as a pre-receptor mechanism: for example, the correction of the chromatic aberration is achieved by the multifocal properties of the lens. By this mechanism, a sharp colour image can be projected onto the retina by a single lens, reducing blur that could not be corrected by accommodation (Malmstrom and Kroger, 2006). In the auditory

system it is the lever action of the auditory ossicle that leads to an amplification of the signal carrier. In the mormyrid electric fish *Gnathonemus petersii,* interaction of objects with the electric field of the fish produce a so-called Mexican-hat effect, giving a centre-surround structure to the object-image at the sensory surface. This effect enhances the acuity of the electric image of an object (Budelli et al., 2002). Pre-receptor mechanisms have also been described for South American weakly electric fish where they modify and shape the local electric signals at various regions of the skin and thus enhance the perception of electric images (Caputi et al., 2002; Migliaro et al., 2005).

Here, we explore pre-receptor mechanisms in *G. petersii*, by investigating the local physical properties of the electric field relative to the body of the fish. It is thus possible to give a detailed description of the local signal carriers and the images projected by nearby objects onto various body regions of the fish and to focus, in particular, on a comparison between body regions that might be used differentially during active electrolocation. These regions are the trunk, the nasal region (region above the mouth and between the nares) and the highly mobile Schnauzenorgan. Based on anatomical results of receptor organ densities and behavioural and physiological studies, the latter two regions have previously been termed electric foveae (von der Emde and Schwarz, 2002), and are in part similar to those postulated for a Gymnotiform electric fish (Castelló et al., 2000). In addition to the physical characterisation of the signal carrier in these regions, we provide data on the density of the electroreceptors in the foveal regions and have used the so-called novelty response (Post and von der Emde, 1999) to measure behavioural thresholds for active electrolocation in the head region. By including physical, anatomical and behavioural data specific to those regions, we give additional evidence for foveation and are able to present data on the different roles of the two foveae during active electrolocation.

MATERIALS AND METHODS

A total of 37 *Gnathonemus petersii* (Günther 1862), ranging in length from 9.7–16 cm, were used in these experiments. Fish were obtained from Aquarélite (Auffargis, France) and from Aquarien Glaser (Frankfurt, Germany) and housed in registered facilities conforming to German, European and international regulations for animal care (European Directive 86/609/EEC and the Treaty of Amsterdam Protocol on Animal Welfare 1997). All experimental procedures were carried out in accordance with the recommendations of the Guide for the Care and Use of Laboratory Animals, Institute of Laboratory Animal Resources, the American Physiological Society's Guiding Principles in the Care and Use of Animals and with the European Council Directive 86/609/EEC and to European Treaties series no. 123.

Experimental set-up: local electric organ discharges and electric images

Anaesthesia was induced by immersion in an aerated solution of etomidate (Hypnomidate; Janssen-Cilag, Neuss, Germany; concentration 16.4 μmol l^{-1} etomidate). Like the previously available anaesthetic metomidate (Hypnodil; Janssen-LeBrun, Paris, France) etomidate does not alter the form or the strength of the natural electric organ discharge (EOD), but the discharge rhythm becomes slower and more regular when compared with the 'awake' state (Engelmann et al., 2006). After loss of postural equilibrium, fish were transferred to the experimental tank and artificially respirated with an aerated solution of etomidate (2.45 μmol l^{-1} etomidate) administered at a flow rate of 40 ml min^{-1} through a tube inserted into the mouth. The water was artificially aerated and its conductivity was maintained constant throughout the experiment (100±5 μS cm^{-1}).

For the measurements of electric images, the fish were supported on a sponge that was located in the middle of an experimental tank (38×27.5×18 cm; L×W×H) and were held upright between two or three pairs of wooden toothpicks. EODs were recorded between a movable silver ball electrode enclosed except for its tip in a glass capillary tube and a fixed indifferent electrode made of Teflon-coated silver wire (0.076 mm) inserted into the back muscle tissue and held in place by a droplet of tissue adhesive (Histoacryl; Braun, Melsungen, Germany). The silver ball electrode was moved in steps of 1 mm around the head of the fish using a micromanipulator. The recorded local EODs (LEODs) were amplified (custom built amplifier; 10×; high pass and low pass cut offs set at 1 Hz and 100 kHz) visualised and stored using a digital oscilloscope (SDS 200A, Conrad Electronics, Hirschau, Germany).

Objects that we used to determine the electrical images were either non-conductive (polyvinylchloride) or conductive (stainless steel and aluminium) cubes (2 cm×2 cm×2 cm) and spheres (diameter=2 cm). Objects were fixed to a wooden rod (diameter=2 mm) and positioned with the help of a micromanipulator. The exact placement of the different objects, 0.25 cm in front of the mouth, was verified by taking a digital photograph at a fixed point exactly above the mouth and by then comparing the images using Photoshop (Adobe) software.

When measuring the properties of the electrical field in the absence of objects, fish were anaesthetised using etomidate (2.45 μmol l^{-1}) in the experimental tank. Under these conditions no artificial respiration was needed as gilling did not stop. This allowed the measurement of the electric field in the absence of the respiration tube. The experimental tank and fish positioning were similar to the previous set-up.

Recording and analysis of the local electric organ discharge

Head to tail EODs (hEOD) were recorded between carbon recording electrodes placed caudal to the tail and rostral to the mouth at the sides of the experimental tank. Differentially measured voltages were amplified (custom built amplifier; 10×; bandpass filter: 1 Hz and 100 kHz) and digitised (Cambridge Electronic Design Power 1401, 16 bit, 625 kHz Analog-Digital Converter; Cambridge Electronic Design Ltd., Cambridge, UK). The hEODs were recorded in all experiments and served as the temporal reference for the measurements described in the section below.

In order to describe the properties of the LEOD, we constructed a quadruple recording electrode comparable to the one described by Castelló et al. (Castelló et al., 2000). The electrode was made of coated stainless steel wire (diameter=0.134 mm) led through a glass capillary. The active electrodes were oriented along the three orthogonal axes of the animal (mediolateral *x*, rostrocaudal *y*, and dorsoventral *z*) while the tip of the fourth electrode served as the central reference (see Fig. 1B). Electrode tips were 4 mm from the reference electrode. The potential differences between the active electrodes and the central reference were amplified using a high input-resistance amplifier (10× differential amplifier AI-410, SmartProbe, Axon Instruments, Union City, CA, USA) band-pass filtered (0.1 Hz to 30 kHz, Cyberamp 380, Axon Instruments), and digitised (CED 16 bit, 250 kHz; Cambridge Electronic Design Ltd). Using Spike2 software (Cambridge Electronic Design Ltd), LEODs were averaged over 6–45 successive LEODs at each position and electrode orientation. The potentials obtained in this manner represent the voltage gradients along the three orthogonal

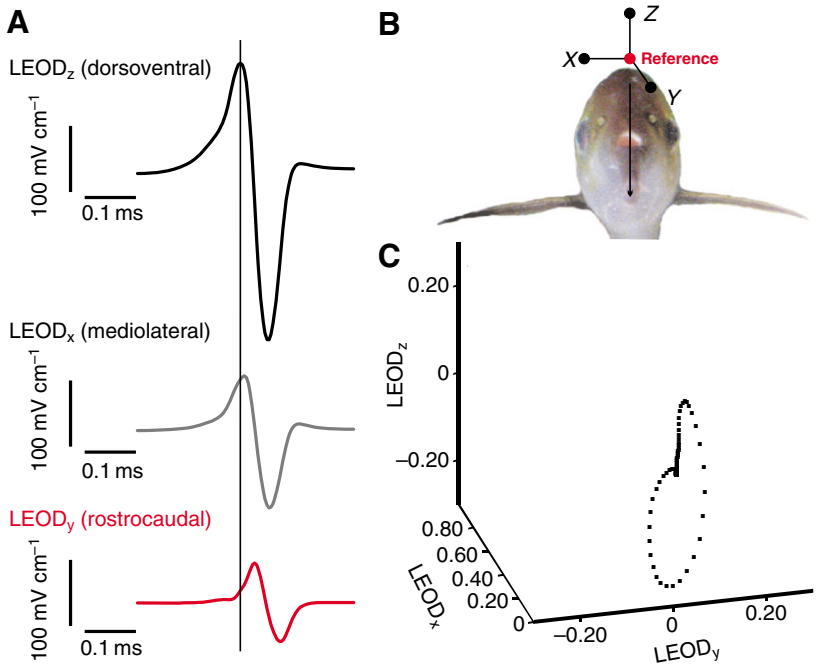

Fig. 1. Explanation of the recording procedure for the vectorial components of the local electric organ discharges (LEOD). (A) An example of the three local electric organ discharges recorded at a position of 50% of the body length. For each orthogonal axis the single LEOD is shown. (B) Each LEOD was recorded using a specialised probe (c.f. text) in the medial plane of the fish (depicted by the black arrow). (C) The time difference of the LEOD in the dorsoventral and rostrocaudal direction (indicated by the black bar in A) results in a vector loop when both LEODs are plotted against each other (data are given in V cm^{-1}).

axes of the animal, hence vectorial addition of the three gradients results in the complete local EOD (LEOD):

$$\text{LEOD} = \text{EOD}_x + \text{EOD}_y + \text{EOD}_z \, . \quad (1)$$

Voltage gradients reported in this paper are all given in V cm^{-1}. In the majority of the experiments the electrode was moved along the rostrocaudal axis at the level of the midline of the fish. The distance to the skin of the fish at each position was adjusted to be 1 mm. For the measurements (N=7 fish; n=7) made at the very tip of the Schnauzenorgan, we artificially moved the Schnauzenorgan between 38° and 72° to the left by using a thin thread attached to its base. After bending the Schnauzenorgan the same types of recordings were done as in all other positions.

For every mean potential, we extracted the amplitude and the direction (angle) of the LEOD vectors by computing the field modulus as a function of time (t):

$$\text{Modulus}\,(t) = \sqrt{[\text{LEOD}_x(t)^2 + \text{LEOD}_y(t)^2 + \text{LEOD}_z(t)^2]} \, . \quad (2)$$

The modulus captures the absolute amplitude of the EOD at a given point in time. The azimuth at any given time is defined as:

$$\text{Azimuth}\,(t) = \arctan[\text{LEOD}_x(t) / \text{LEOD}_y(t)] \, . \quad (3)$$

The amplitude and direction of the LEOD vector was calculated with these formulas for the maximum peak of the modulus to obtain the direction of the field vector relative to the skin. In addition, we plotted the local orthogonal components of the LEOD, i.e. the individual voltage gradients for the x, y and z electrode as vector trajectories. These vector trajectories were constructed by plotting one local orthogonal potential as a function of another local orthogonal potential (cf. Fig. 1C). Therefore, they represent the amplitude and direction of the local field vector. All calculations were done using either Excel or MatLab.

Recording and analysis of the electric images

For each object, measurements were performed in a horizontal plane at the height of the snout, a second horizontal plane 5 mm above the snout and in the medial plane. At each point, ten EODs were recorded in the absence of an object, giving the LEOD, and in the presence of an object, giving the local distorted EOD (LdEOD). EOD data for electric images are given in volts (V). In order to calculate the distance between electrode positions, x, y and z coordinates of the electrodes were noted and the Cartesian distances between different measuring positions were computed.

The dimensionless voltage modulation caused by the object at a given position on the skin was determined as:

$$\text{Modulation} = \text{LdEOD} / \text{LEOD} \, . \quad (4)$$

In addition, we determined the voltage difference between the undistorted EOD and the distorted EOD at each point:

$$\text{Difference} = \text{LdEOD} - \text{LEOD} \, . \quad (5)$$

These measures were used to construct the electric images, i.e. the spatial profile of changes of the electric field at the fish's skin caused by an object (Caputi et al., 1998; Rasnow, 1996). The slope of the images was measured after normalising: the highest modulation was set to 1 and the lowest value was set to 0. The first four data points around the peak of each electric image were used to calculate the slope because this is the region of the highest slope values (Fig. 7D).

As a control, we recorded ten EODs at a reference position at different times during the experiment in the absence of an object. These measurements were used to determine the stochastic variation between different measurements and served as the no-object baseline. To discriminate between the baseline and the electric image we tested every single point of the images by using a univariant analysis of variance (ANOVA) with the Games-Howell *post-hoc* test. The width of an electric image was estimated as the distance between the first and the last positions where significant differences between the recorded modulation and the baseline occurred. Electric images obtained with different objects were also compared using a univariant ANOVA.

Distribution of electroreceptor organs

Anatomical data about electroreceptor organs were obtained using methods previously described (Bacelo and Grant, 2001). Briefly,

flat-mount preparations of the skin regions (Harder, 1968; Harder et al., 1967), were stained with Toluidine Blue, which gives differential staining of the different electroreceptor organ types, and the densities of these receptor organs were determined (N=23 fish).

Measuring the novelty response

Animals were anaesthetised by immersion in MS-222 (tricaine methane sulfonate; Sigma, St Louis, MO, USA; concentration 306.17 μmol l^{-1}) and transferred to a Perspex™ holder. In this holder, the fish's trunk was supported lightly between two Perspex™ meshes that were covered with foam rubber, and the head of the fish was free rostral to the operculum. The holder was situated in a tank measuring 30 cm×19.5 cm×18.5 cm (L×W×H). Anaesthesia was then discontinued and the fish recovered within a few minutes. The water conductivity in the tank was constant at 123±1 μS cm^{-1}. The EOD of the fish was recorded by a pair of carbon electrodes placed on the inside wall of the tank at the head and tail of the fish (custom built amplifier, 10 Hz to 10 kHz band-pass filtered) and stored using the CED digitiser (Cambridge Electronic Design Micro 1401 12 bit, 200 kHz, analogue–digital converter) and Spike2 software (Cambridge Electronic Design Ltd). A novelty response consists of a transient acceleration of the rate of EOD evoked by a sudden sensory novelty (Ciali et al., 1997; Post and von der Emde, 1999; Szabo and Fessard, 1965).

A pair of passive dipole objects (Fig. 12A) was placed in the tank perpendicular to the fish at several different distances from the skin. These dipoles were positioned at several different body regions of the fish (the tip of the Schnauzenorgan, the middle and base of the Schnauzenorgan, the eye and the middle of the operculum). The resistivity of the objects could be switched from a short circuit to an open circuit in order to evoke novelty responses of the fish. At the instant of switching a triggering signal was recorded in Spike 2.

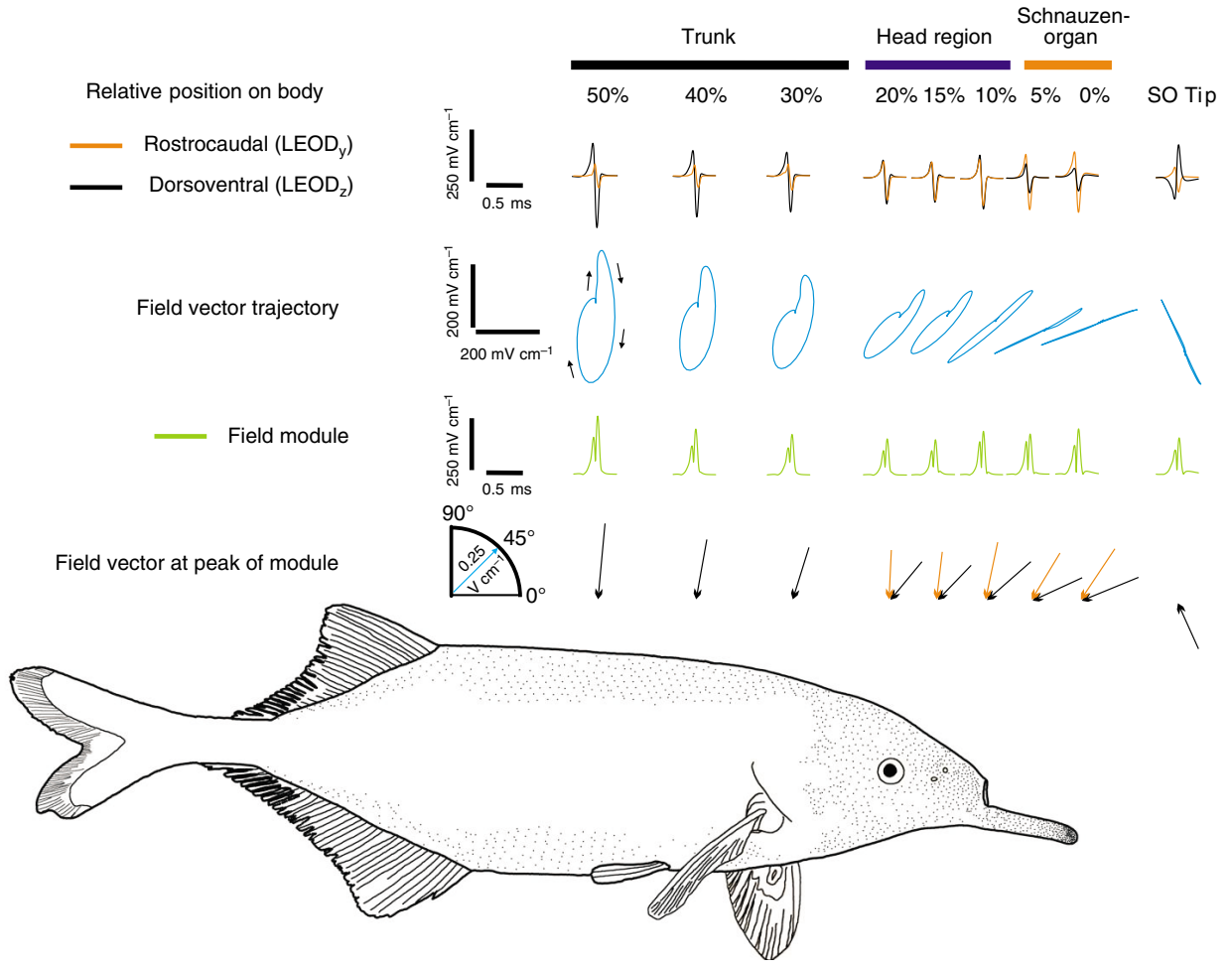

Fig. 2. Example of the LEOD measurements obtained from a single fish. All data shown are averages of 15 consecutive measurements. The position relative to the length of the fish is given in the topmost row; the LEOD components (z and y) are shown in the second row. The field vector trajectory of the *z* and *y* LEOD is depicted in blue in the third row. At the 50% position, the direction of rotation of the vector loop is shown as an example. Note that the LEODs at the nasal region and the Schnauzenorgan (SO) are highly in phase, which can also be seen in the individual field components of the *z* and *y* data shown in black and orange in the second row. The fourth row shows the field module of all three LEODs. In the bottom row, the field vector calculated at the peak of the field module is shown, i.e. the vectors represent the effective stimulus strength and direction. Here, black arrows indicate the vectors as determined relative to the *x*, *y* and *z* plane. Orange arrows are identical to the black vectors, except that their angle is given with respect to the sensory surface of the fish. The drawing of the fish is aligned to match the relative body positions where measurements were taken. Note that the electric organ is situated in the caudal peduncle before the tail fin. Each dot in the drawing indicates the location of an individual mormyromast, showing that the density is highest at the Schnauzenorgan.

Novelty responses were determined by the following method. The mean interval and the standard deviation were calculated for the 20 EODs prior to a switch. The mean interval value was subtracted from all EOD intervals, and the result was divided by the standard deviation (Hall et al., 1995). The resulting *Z*-transformation of the data provided us with a statistical measure for the quantification of the amplitude of the novelty responses (Fig. 12A). A novelty response typically consisted of a decrease of the duration of the EOD intervals and such a decrease lead to negative *Z*-values. For convenience, we transformed the data in such a way that they are presented as positive values. Based on latency and amplitude of novelty responses, spatial sensitivity profiles were constructed in Matlab.

RESULTS

Previous work, limited to the trunk region of the fish, showed that electric images contain information on the shape and material of nearby objects (von der Emde and Schwarz, 2002). More recent anatomical work (Bacelo and Grant, 2001; Hollmann and von der Emde, 2004; von der Emde, 2006) showed that the Schnauzenorgan and possibly the nasal region are of major importance for object localisation. Here, we fully characterise the properties of the local EOD at different regions of the skin including the Schnauzenorgan. Next, we compare electric images between different regions of the body, and finally we examine anatomical and behavioural evidence for the specialisations of the Schnauzenorgan and the nasal region.

Vectorial components of the local EOD

In order to characterise the electric field properties, we measured the LEODs close to various body regions of the fish. The LEOD was obtained by measuring its vectorial components in the three orthogonal planes (*x*, *y*, *z*) at fixed positions along the midline of the fish close to the skin. Fig. 2 shows the *y* and *z* components of the LEOD obtained in this manner (second row). The data were highly reproducible from one experiment to the next (N=7 fish). Only the orthogonal components *y* and *z* are discussed here, because the *x* component is negligible when measured at the midline. We found that the phase relationship of the $LEOD_y$ and $LEOD_z$ is almost constant throughout the EOD (Fig. 2, third row from the top) from the Schnauzenorgan to the head (20% of body length). On the trunk, however, the orthogonal components varied in their phase-relationships, and consequently the angle of the current vector changed during the EOD.

The angle and amplitude of the current vector was analyzed at the time of the positive peak of the LEOD using the modulus (fourth row from the top in Fig. 2). Its inclination varied systematically along the length of the animal (Fig. 2, bottom) but was of almost constant amplitude (see Fig. 2, bottom). At any given position the inclination was constant in all experiments performed with different fish, which is reflected in the finding that the mean angles (N=7) at each position were significantly different from a random distribution (Rayleigh test: all *Z*-values >6, P<0.001). For this reason we only show the general properties of the LEODs for one fish in Fig. 2.

As stated above, the directions of the mean vector deviated significantly along the axis of the fish (Fig. 2, bottom). For example, the mean angle on the trunk was close to 80°. When measured at the head, this angle gradually decreased until it reached its lowest inclination at the Schnauzenorgan. When passing the tip of the Schnauzenorgan (electrode configuration is shown in Fig. 5), the direction of the vector changed such that it was now directed almost directly towards the tip. As these angles are given with respect to the orthogonal measuring planes, we transformed them with respect

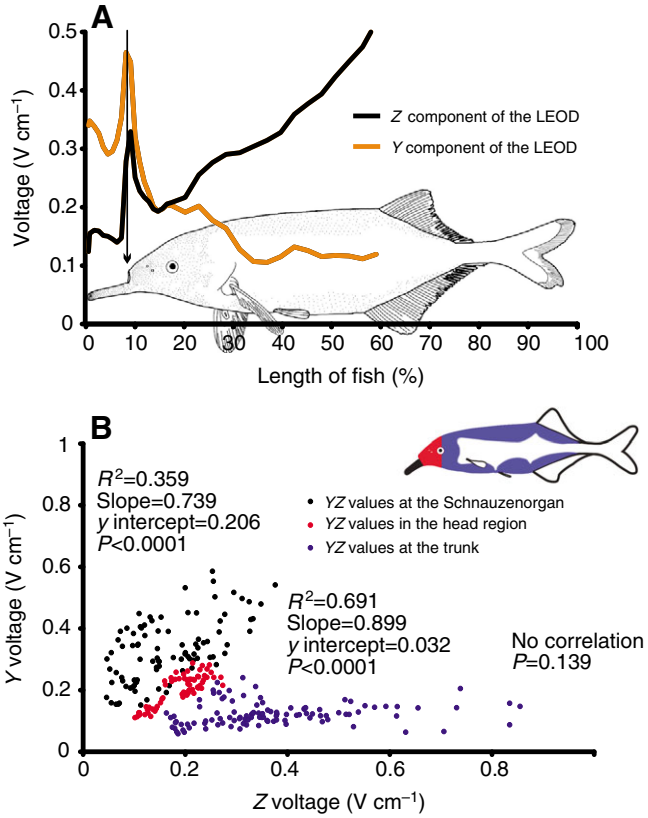

Fig. 3. (A) The peak-to-peak values for all measured positions of the rostrocaudal (orange trace) and dorsoventral (black trace) EOD components. At the trunk of the fish, the dorsoventral component is prominent but at the Schnauzenorgan the rostrocaudal component dominates. In the head region only, both components are similar in their contribution to the LEOD. Note that the fish's constantly open mouth leads to an increase in the amplitude of both components at the head region (black arrow). (B) Plot of the peak-to-peak values in the different body regions. The *z* component is plotted *versus* the *y* component of the LEOD. Note that at the head region (red dots) the influence of both components is similar.

to the sensory surface. This is the angle relevant for the receptors (orange arrows in Fig. 2, bottom row). Now, the head and trunk directions are comparable, i.e. the electrical current is directed towards the sensory skin surface at almost 90°. By contrast, at the Schnauzenorgan the current inclination is 45°.

This change in current flow direction is associated with a change in the relative strength of the LEOD components. At the trunk, the LEOD in the dorsoventral direction is strongest. At the head both components are of equal strength (Fig. 3A and Fig. 2 second row from top). However, rostral to the opening of the mouth, it is the $LEOD_y$ that contributes the most to the LEOD. The dramatic change in the current direction between the body (almost 90°) and the Schnauzenorgan (45°) is most likely due to the opened mouth and the tip-effect caused by the conic shape of the head.

By comparing the ratio between the peak-to-peak (p–p) voltages measured along the trunk, the head and the Schnauzenorgan for the *z* and *y* components of the LEODs (Fig. 3B), the change in the relative contributions of the LEOD components can be quantified. For all measured positions at the head the ratio of the two components is one; however, this ratio is significantly bigger at the Schnauzenorgan (comparison of the slopes; *t*-test, N=157; d.f.=153; t=1.941, P<0.05). This confirms that rostral to the mouth it is the

y component of the LEOD that dominates (comparison of elevation; *t*-test, N=157; d.f.=154; t=8.11, P<0.001). For the trunk, as expected from the constancy of the z component, there was no significant correlation between the two components for all measured positions, which prevented us from comparing the trunk with the other two body regions (Fig. 3B).

Spatial variation of the LEOD

For the analysis of the spatial variation of the signal carrier we calculated the coefficient of variance for the positive and negative peak of the EOD. No significant differences between the body regions were found. The coefficient of variation was –0.07±0.04 at the trunk, –0.07±0.03 in the head region and –0.1±0.03 at the Schnauzenorgan. The variation hence is smaller, regardless of the region investigated, than that reported for *Gymnotus carapo* (0.18±0.04 at the fovea and 0.21±0.05 at the parafovea), another species from South America for which similar investigations were performed (Castelló et al., 2000). Thus the detection of waveform distortions is not limited to distinct regions of the body at the pre-receptor level. At a central processing level, however, a difference between body regions occurs for the Schnauzenorgan, where the representation of waveform sensitive B-mormyromasts is higher in the electroreceptive lateral line lobe (ELL; see Discussion for details).

Although the EOD waveform is remarkably constant over the whole of the fish's body, there is a difference in the amplitude between the body regions: constant amplitudes of the LEOD were only found in the head region. A way to visualise the constancy of the electric field at the head is shown in Fig. 4. Here we plotted the amplitude of the LEOD measured with a single electrode referenced against an internal electrode in the fish's muscle tissue (see Materials and methods). Measures obtained along the midline and along the two horizontal planes are almost constant within the nasal region. Beyond this region, amplitudes decline caudal to the nares of the fish. In order to quantify these findings, we again measured the coefficient of variation for all measures in the horizontal plane (N=12). Within 15 mm around the snout the coefficient of variation was 0.023±0.007. Caudal to this region the coefficient of variation was higher (0.063±0.019), i.e. the voltage distribution is less constant. This difference was significant (paired samples *t*-test, N=12; d.f.=11; t=7.087, P<0.0001), i.e. the electric field is homogeneous in the nasal region and non-homogeneous caudally (Fig. 4).

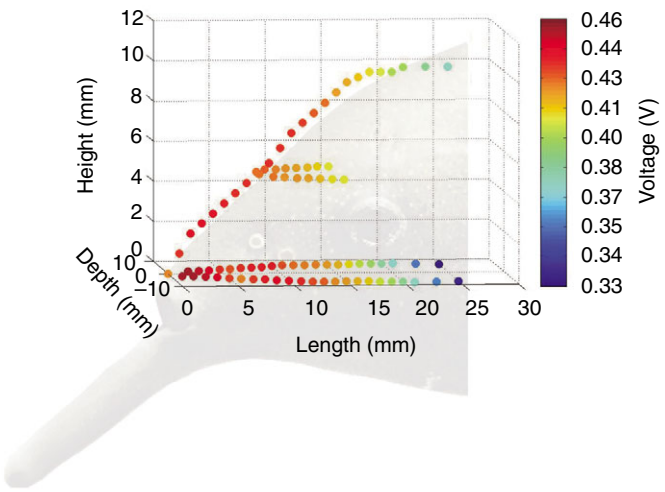

Fig. 4. Colour-coded peak-to-peak distribution of the LEOD amplitude at the head as measured with a single electrode referenced against the internal tissue. Note that the EOD amplitude is fairly constant over the nasal region and only changes further caudally.

Steadiness of the electric field during movement of the Schnauzenorgan

The modification of the field by the Schnauzenorgan is of extreme importance because the Schnauzenorgan is moved constantly during foraging. One might expect that motion of the receptive surface of the Schnauzenorgan would lead to changes in the sensory stimuli experienced by the electroreceptors (e.g. Bastian, 1995), which the animals would need to take into account when analysing the environment. Alternatively, motion in itself might not alter the field properties relative to the sensory surface and hence not impose additional problems for electrolocation. Here we tried to assess these two possibilities by moving the Schnauzenorgan laterally and comparing the field properties before and after the movement (Fig. 5).

The amplitude of the EOD decreased dramatically, by 80%, when the Schnauzenorgan was bent by approximately 62° (±13.5°; mean ± s.d., N=7, n=7) to the left while keeping the recording electrode stationary (Fig. 5, compare position I with position II). However, the initial amplitudes were restored when measuring the field at the new tip location (Fig. 5, position III). This demonstrates that the internal conductivity of the Schnauzenorgan forces the electric field to 'move' with it during bending. As a consequence, the local sensory stimuli (the LEODs) at the Schnauzenorgan's tip do not change when the fish moves.

To show that the tip-effect is a local effect and that it is limited to the very tip of the Schnauzenorgan we repeated the experiment

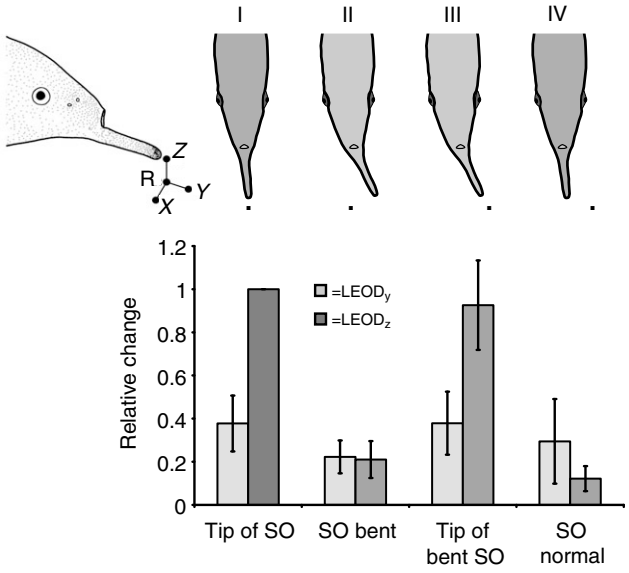

Fig. 5. Effect of movement of the Schnauzenorgan (SO) on the amplitude of $LEOD_y$ (light grey bars) and $LEOD_z$ (dark grey bars). Dots represent the electrode positions. In position I, mean amplitudes (N=7) normalised to the peak-to-peak amplitude of the $LEOD_z$ are shown, measured at the tip of the Schnauzenorgan in a normal position. At II, the Schnauzenorgan was bent to the left by 62±13.5° whereas the LEODs were recorded at the same site as in I. The initial amplitudes could be recovered by readjusting the recording position to the new tip-position (III), while a subsequent return of the Schnauzenorgan to its normal position without moving the recording electrodes decreased the amplitudes again (IV).

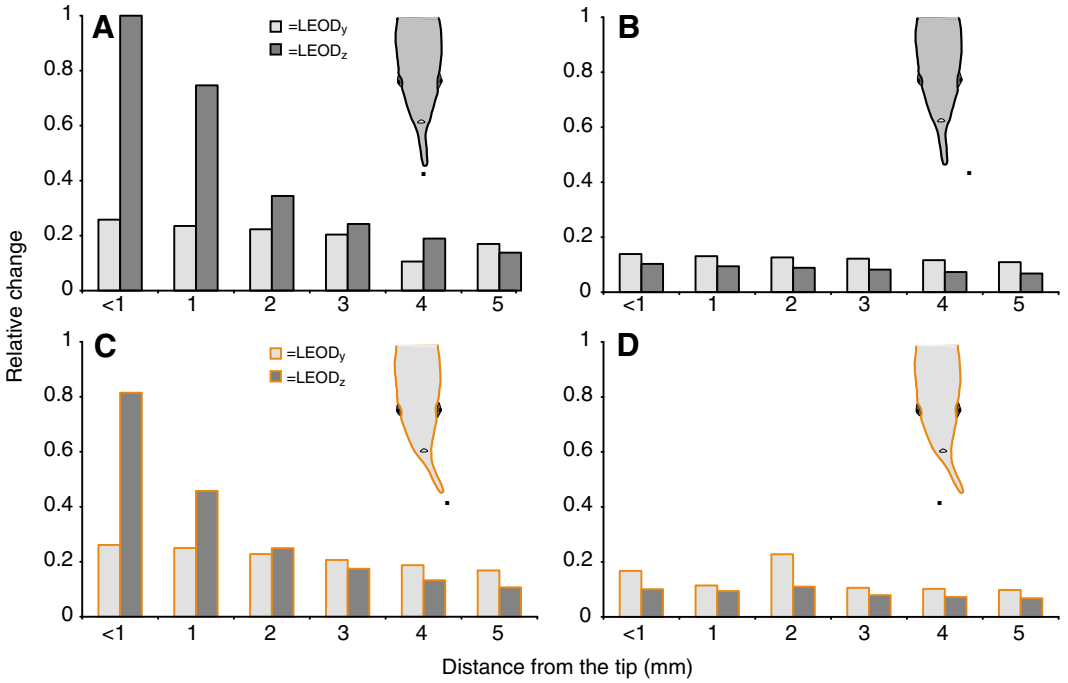

Fig. 6. The 'tip-effect' on the amplitude of $LEOD_y$ (light grey bars) and $LEOD_z$ (dark grey bars) as a function of distance. The distance between the Schnauzenorgan and the recording electrode was varied from less than 1 mm to 5 mm. (A) The Schnauzenorgan is in its normal position and the probe (black dot) is in front of the tip. (B) The Schnauzenorgan is in its normal position and the probe is positioned left of the tip. (C,D) The same probe conditions as in the top row but with the Schnauzenorgan bent to the side (depicted in red) (cf. Fig. 5).

described above but varied the distance between the tip of the Schnauzenorgan and the probe. As shown in Fig. 6A,C the tip-effect is high at the very tip of the Schnauzenorgan. As in the previous experiments, the EOD amplitude decreased if the Schnauzenorgan was bent (Fig. 6D) or the electrode was moved away (Fig. 6B). When the distance between the electrode and the Schnauzenorgan was increased, the amplitude of the z-LEOD decreases. At a distance of 5 mm, the effect is almost gone. In the conditions where the electrode was not in front of the Schnauzenorgan no changes occurred with increasing distance and the level of the LEOD was constantly low (cf. Fig. 6B,D).

Electric images at the head, the trunk and the Schnauzenorgan

Electric images have been studied in detail at the trunk of *Gnathonemus petersii* (Budelli et al., 2002; Caputi and Budelli, 2006; Schwarz, 1997; Schwarz, 2000; Schwarz and von der Emde, 2001; von der Emde, 2006). To test our hypothesis that the nasal region is specialised for a precise image representation, and hence ideal for electrolocation, electric images of cubes and spheres were measured in this area. For each object described in the following section, three individual electric images were taken independently. An example of the voltage distribution on the skin in the presence and absence of a metal cube is illustrated in Fig. 7A.

Three transformations were applied to the raw data. First, we calculated the differences in amplitude of the LEODs in the presence and in the absence of the object (Fig. 7B). This is a measure of the absolute impact of an object in the electric field. To relate the local distorted electric organ discharge to the undistorted local electric organ discharge we secondly used the term modulation, which is the relative impact of an object in the electric field (Fig. 6C). This gave us a measure to compare each electric image. Third, we normalised the electric images to pool and compare the results of the single experiments. We used this transformation to calculate the slope of the electric images.

In general, image widths (see Materials and methods) were smaller for the spheres than for the cubes, regardless of the objects' material (Table 1). For objects that only differ in material, non-conductive objects gave smaller images than conductive objects. For all cases (sphere, cube, metal, plastic) an individual plot of the recorded modulation is shown in Fig. 8. It shows the electric images of all objects in the three measuring planes with the modulation coded in colour. Note that the images are symmetrical and that the highest modulation values as well as the highest slope values were found in the nasal region. These parameters have been shown to be those mostly probably used for shape and distance detection in *G. petersii* (von der Emde, 2006).

However, compared to the data published on electric images on the trunk, amplitude modulations never fell below 1 for the metal cube or exceeded 1 for the plastic cube. This means that the metal cube caused only amplitude increases but no decreases, and correspondingly the plastic cube caused only amplitude decreases.

Table 1. Mean width (mm) of the recorded electric images in the different measuring planes (horizontal 1, medial and horizontal 2)

Objects	Horizontal 1	Medial	Horizontal 2
Metal cube	32.03±5.82	18.13±1.96	20.26±3.13
Metal sphere	28.61±2.14	11.96±2.22	11.99±3.63
Plastic cube	21.47±5.27	14.85±5.96	8.4*
Plastic sphere	18.17±3.32	8.34±2.12	7.11±2.06

Values (mm) are mean ± s.d.
*Only one measurement was performed in this plane with a plastic cube.

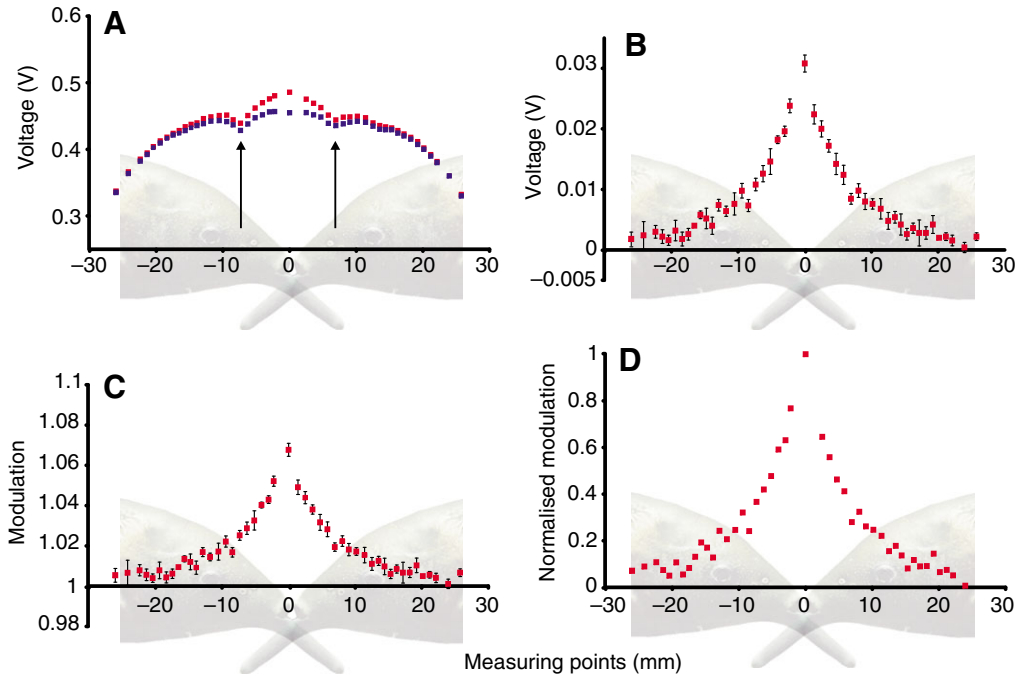

Fig. 7. (A) The voltage distribution (peak-to-peak amplitude of the LEOD) on the skin, measured in the presence (red squares) and absence (blue squares) of a metal cube. Each symbol represents the average of ten LEODs. The abscissa shows the plane where the voltages were measured along the fish at the left and right side of the mouth, with 0 indicating the position of the mouth. Note the relatively stable voltage distribution in the range from –15 to +15 mm (the arrows indicate the distortions caused by the nostrils). (B) The resulting voltage difference caused by the presence of the metal cube. (C) The modulation of the voltage due to the presence of the object. (D) Normalised modulation (maximum set to 1), which was used to calculate the slope of the electric images. In B and C, values are means ± s.d. (N=10).

Accordingly, the Mexican-hat profile (Coombs et al., 2002; Gómez et al., 2004; Schwarz, 2000) of the images did not appear at the head.

A comparison of the electric images of the different objects is shown in Fig. 9. The points of the electric images represent the mean of the three individual measurements. Each point is therefore the average of 29–30 EODs. Regardless of the objects' material, the profile of the electric images of cubes and spheres differed (metal cube *vs* metal sphere: horizontal 1: ANOVA, N=2754, F=7.61, P<0.001; medial: ANOVA, N=1318, F=9.64, P<0.001; plastic cube *vs* plastic sphere: horizontal 1: ANOVA, N=2578, F=12.29, P<0.001; medial: ANOVA, N=1019, F=17.07, P<0.001).

The comparison of electric images caused by objects of different conductivity shows that the absolute value of modulation differs: the field distortion is greater for conductive objects than for non-conductive objects. The electric images of identically shaped objects that differ only in their resistivity are in our case no simple mirror images. This finding corresponds to modelling results (Sicardi et al., 2000). Based on this model, it was found that the slope of the electric images depended on the object's shape. We got similar results, but in contrast to Sicardi et al., we found that in the nasal region the slope of the image caused by the sphere was greater than the slope of the image caused by the cubes (Table 2; cubes *vs* spheres: independent samples t-test, N=36, d.f.=34, t=6.88, P<0.001). Image slope neither depends on the material (metal cube *vs* plastic cube: independent samples t-test, N=18, d.f.=16, t=0.542, P=0.595; metal sphere *vs* plastic sphere: independent samples t-test, N=18, d.f.=16, t=–0.322, P=0.751) nor on the plane in which the image was measured (cubes, horizontal 1 *vs* medial: independent samples t-test, N=18, d.f.=16, t=–1.497, P=0.154; spheres, horizontal 1 *vs* medial: independent samples t-test, N=18, d.f.=16, t=–0.28, P=0.783).

The energy source for the electric image is internal to the fish and because no current can be generated de novo by the object, the increased (decreased) LEOD amplitudes in certain regions of the overall field need to be balanced by reduced (increased) amplitudes at other skin areas. As we could not measure such effects in the head region, we repeated our measurements with a paired electrode measuring the y component of the local electric signal, including the Schnauzenorgan in this study. In this recording configuration the previously apparently missing voltage 'drain' was indeed found at the Schnauzenorgan (Fig. 10A,B). As might be expected based on the strong contribution of the y component to the LEOD at the Schnauzenorgan, the effect was most prominent when the $LEOD_y$ was measured, but it was also present on a weaker scale in the z-plane.

Table 2. Mean slopes of the electric images in the different planes (horizontal 1 and medial)

Objects	Horizontal 1	Medial
Metal cube	0.11±0.018	0.1±0.012
Metal sphere	0.14±0.016	0.14±0.012
Plastic cube	0.11±0.016	0.09±0.016
Plastic sphere	0.15±0.027	0.14±0.018

Data are means ± s.d. of 6 values for each object in the horizontal plane and 3 values for each object in the medial plane. For the horizontal data the slope was calculated for the left and right side independently. Pooling of the resulting values was possible because the images were symmetrical.

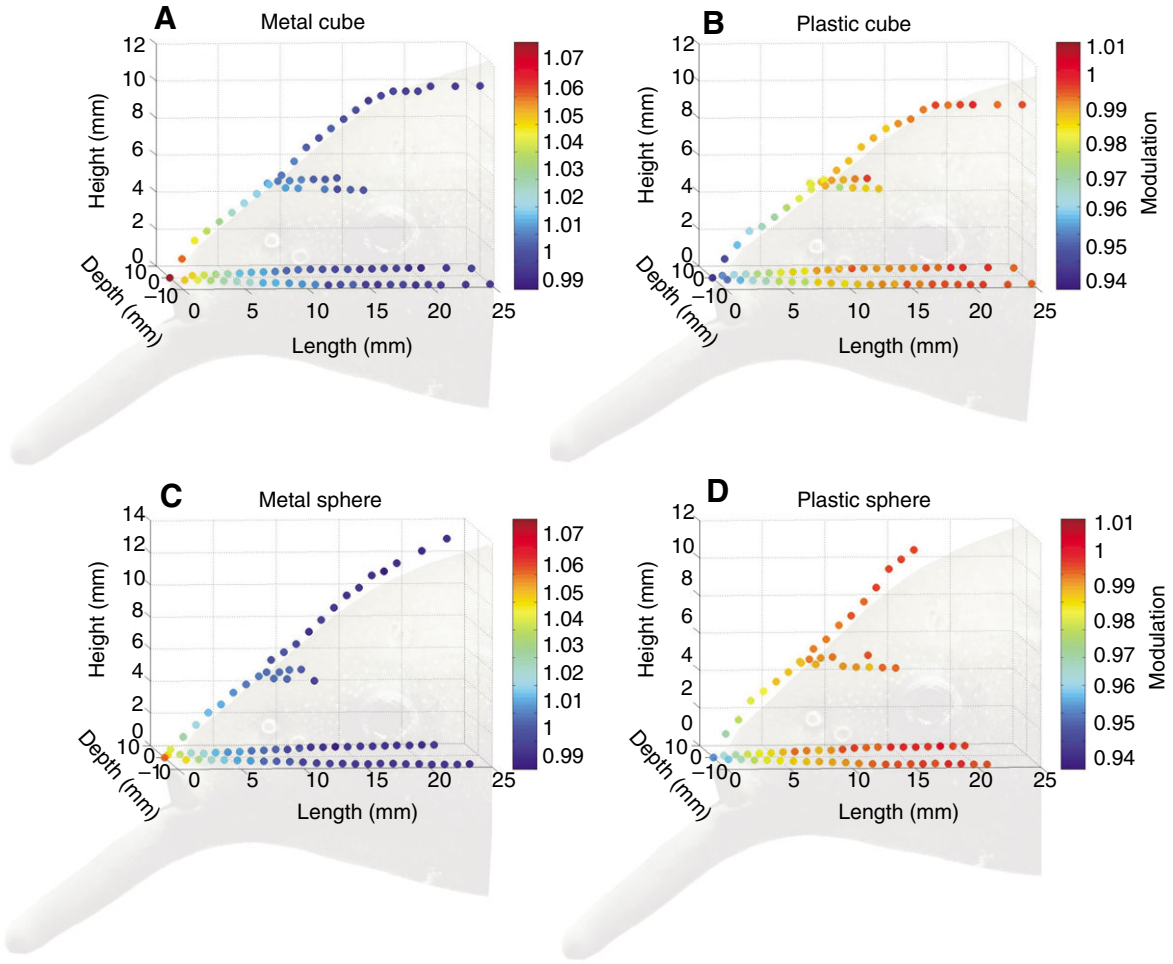

Fig. 8. Three-dimensional comparison of the electric images of different objects, with the modulation caused by the object colour coded. (A) The electric image of a metal cube. (B) The electric image of a plastic cube. (C) The electric image of a metal sphere. (D) The electric image of a plastic sphere. Note that high modulation values are shown in red and low modulation values are shown in blue. Therefore, the baseline for conductive objects (metal) is shown in blue and the baseline for non-conductive objects (plastic) in red.

Distribution of electroreceptor organs

The distribution of electroreceptor organs differs in the different body regions mentioned above. It is highest at the tip of the Schnauzenorgan (Fig. 11A) and decreases towards its base to a value that is still high compared to other body regions. The second highest density of mormyromasts was found in the nasal region (Fig. 11B). The density of electroreceptors is significantly higher at the Schnauzenorgan and in the nasal region compared to the trunk.

Because of the funnelling and the tip effects, the current flow at the tip of the Schnauzenorgan is such that objects positioned in front of the tip should influence the mormyromasts most strongly. This, seen together with the receptor distribution, suggests that the Schnauzenorgan and especially its tip should have the highest sensitivity to changes in the electric field caused by objects and that the spatial resolution of the active electrosensory system would be greatest here.

Behavioural sensitivity

In order to test the above hypothesis, we used the novelty response, which is a transient acceleration of the rate of electric organ discharges in response to a sensory novelty (Szabo and Fessard, 1965). Novelty responses were evoked by a sudden change of the electrical resistance of a dipole object placed at different positions along the body of the fish (Fig. 12A). The amplitude of the novelty response can be considered as an indicator of the local sensitivity, as has been shown in detail for *Gymnotus carapo* (Aguilera and Caputi, 2003). A similar relationship between stimulus intensity and the novelty response was found in mormyrid fish too (Ciali et al., 1997; Post and von der Emde, 1999). The novelty response amplitudes were highest when the dipole object was facing the tip of the Schnauzenorgan (Fig. 12B). When the object was placed to the side of the tip, sensitivity decreased, and it decreased even further at more caudal object positions. This decrease from the tip to the head was significant up to a lateral distance of 7 mm (Spearman-Rho, one-tailed: $P<0.039$). At a distance greater then 12 mm novelty responses could only be evoked occasionally, adding support to the importance of the tip-effect at the chin appendix.

Although this behavioural measure cannot be used to determine whether the increase in sensitivity was caused by the pre-receptor mechanisms described above or by the higher receptor density, it clearly shows the relevance of the electrosensory fovea of the Schnauzenorgan tip.

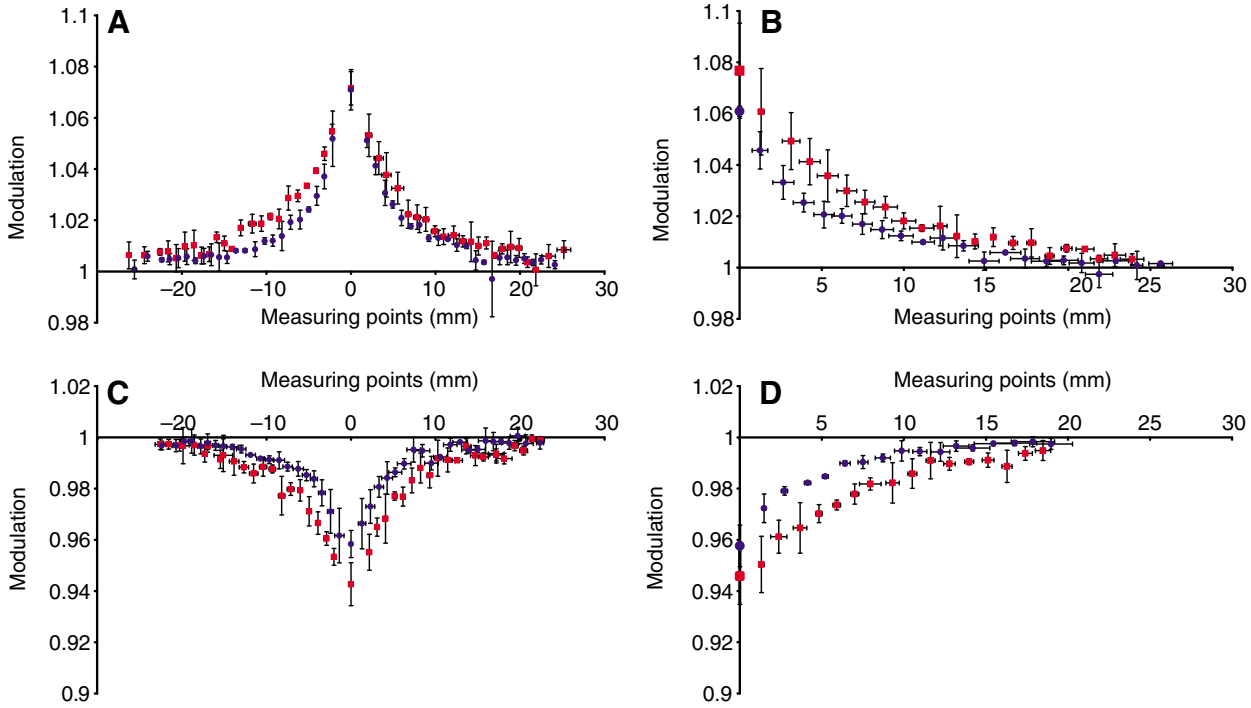

Fig. 9. Comparison of the electric images of different objects. (A) Modulation of metal cubes (red squares) and metal spheres (blue circles) in the horizontal plane. Each point represents the mean of three measurements. (B) The same comparison in the medial plane. (C) Comparison of the modulation resulting from a plastic cube (red squares) and a plastic sphere (blue circles). (D) The same comparison in the medial plane.

DISCUSSION

In this paper we show that passive pre-receptor mechanisms enhance the signal carrier for electroreception (local EOD) both in strength and suitability for active electrolocation in *Gnathonemus petersii*. Measurements of the local electric fields, electric images, receptor organ densities and the behavioural sensitivity thresholds all show that the nasal region and the Schnauzenorgan are specialised body regions for active electric sensing. These peripheral, physiological and anatomical specialisations can be regarded as evidence of the existence of two separate foveae: one on the Schnauzenorgan and one on the nasal region.

Evidence of foveation based on the distribution of electroreceptor organs and pre-receptor effects were also shown for two gymnotiform electric fishes, *Gymnotus carapo* (Caputi and Budelli, 2006; Migliaro et al., 2005) and *Apteronotus leptorhynchus* (Rasnow and Bower, 1996). In *Gymnotus carapo*, an electric fish lacking a chin appendix, a foveal and parafoveal region at the head of the animals were distinguished (Caputi et al., 2003; Caputi et al., 2002). This contrasts with *Gnathonemus petersii* where it was proposed (von der Emde and Schwarz, 2002) that the Schnauzenorgan and the nasal region can be considered as two separate electric foveae with different functions: a short-range food classification/detection

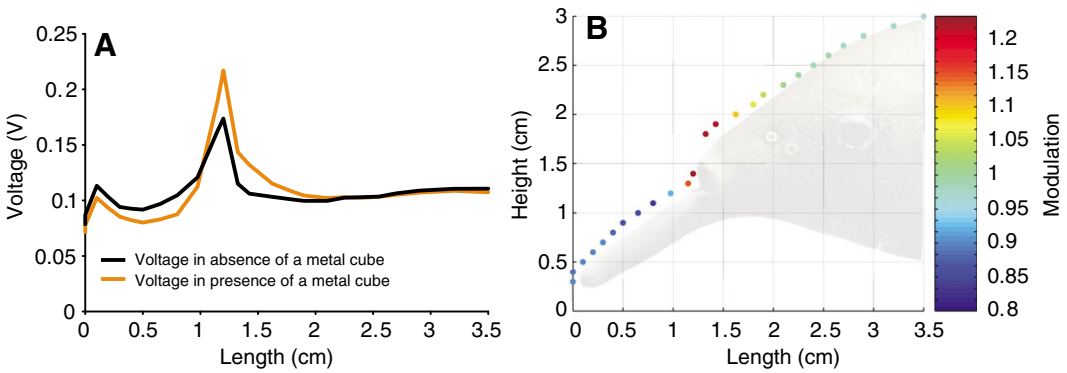

Fig. 10. (A) LEOD amplitudes ($LEOD_y$) measured along the midline of the fish in the presence (orange line) or absence (black line) of a metal cube placed in front of the animals mouth at the same distance as in the other experiments (distance to skin, 0.25 cm). (B) Colour-coded voltage modulations plotted along the midline of a fish, from the tip of the Schnauzenorgan to the head. Modulations <1 (a decrease in voltage caused by the object) are drawn in dark blue and were found only at the Schnauzenorgan. The modulation caused by the object changes at the snout of the animal. At the nasal region, voltages are increased, which cause modulation values >1 (depicted in red).

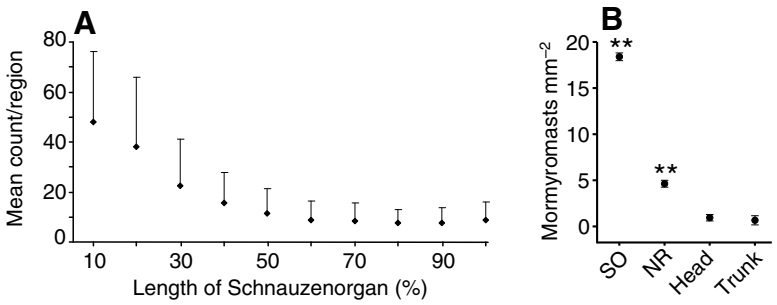

Fig. 11. (A) Mean count of mormyromasts (N=20) in successive bins each representing 10% of the total length of the Schnauzenorgan (SO), showing s.d. only in the positive direction. (B) Mean density of mormyromasts (N=3) for different body regions. Note that the nasal region (NR) contains the second highest density of mormyromasts. Differences in densities were tested with the Student–Newman–Keuls *post-hoc* test: $^{**}P<0.001$.

fovea (Schnauzenorgan), and a far-range object detection and guidance system (nasal region) (Castelló et al., 2000; von der Emde, 2006). The present results support this idea of two separate foveae in *Gnathonemus*. In order to justify this claim, some considerations should be given to the use of the term fovea.

Today the term fovea is often used when describing specialised zones of high (spatial) acuity within a sensory surface, for example the fovea of the eye or the tactile fovea of the star nosed mole, which contains the highest density of tactile receptors (Catania and Remple, 2004). Regardless of sensory modality, all foveae described so far share at least some characteristics: (1) morphological specialisations that can involve pre-receptor mechanisms; (2) a specialised zone of the receptive mosaic with an unusually high density of receptors; (3) a disproportionately high central representation; and (4) specific behavioural strategies that approach or align the fovea to an object or sensory stimulus under investigation (Azzopardi and Cowey, 1993; Azzopardi and Cowey, 1996; Caputi, 2004; von der Emde and Schwarz, 2002).

With regard to these characteristics, both *Gnathonemus* and *Gymnotus* possess foveae. However, an increased receptor density within a spatially confined part of a sensory surface alone is not enough to call a certain part of a sensory epithelium a fovea. This was the reason why the dorsal region of the snout in *Gymnotus* was described parafovea instead. In *Gnathonemus*, however, our data support the hypothesis that these animals really have two separate foveae. First, both for the nasal region and for the Schnauzenorgan, we could show that separate pre-receptor mechanisms exist. At the nasal region, these pre-receptor mechanisms seem to balance the EOD amplitude to be almost uniform. The direction towards the sensory surface is constant (collimation effect) (Castelló et al., 2000) and the vectorial components of the LEOD are of equal strength. This makes the signal carrier equally sensitive to objects located in all three axial spatial dimensions. At the Schnauzenorgan, funnelling of current together with the tip-effect ensure high amplitude EODs at the tip, which are not affected by the scanning movements of the chin appendix. The angle of the field vector at the Schnauzenorgan

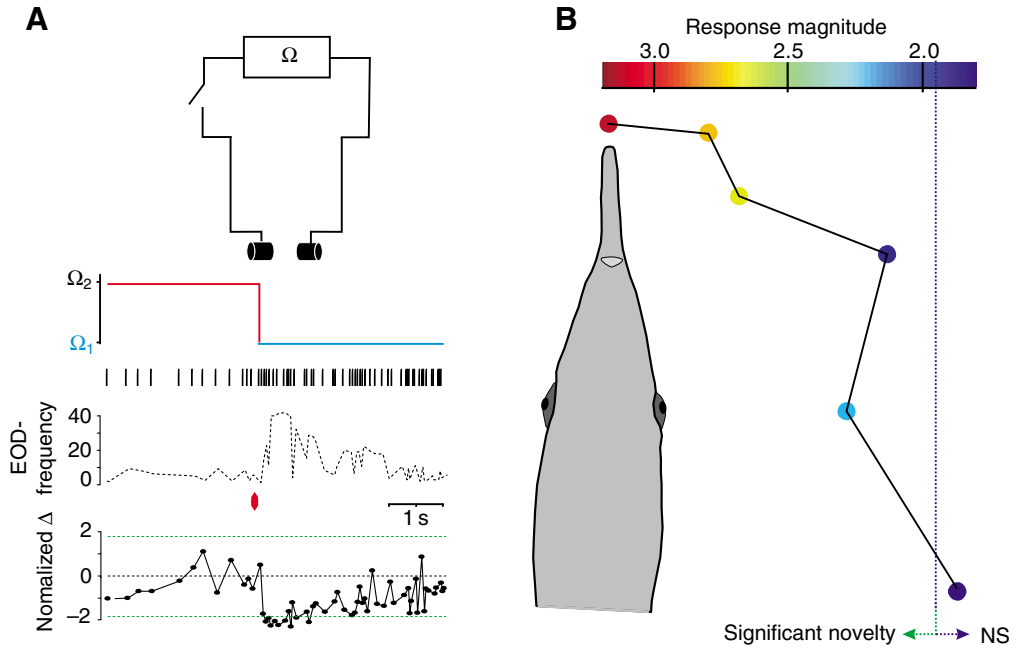

Fig. 12. (A) Schematic of the set-up and method to determine the amplitude Ω of the novelty response. A dipole object of variable resistance was suddenly switched from a high to a low resistance or *vice versa*. The EOD frequency was monitored in response to the switch (see arrow). Several trials with identical switches and identical positioning of the dipole objects were normalised (normalised Δ) by subtracting the mean frequency and dividing by the variation of the 20 EODs prior to a switch. Note that negative values in the normalised data correspond to an acceleration of EOD frequency and that this measure is transformed to positive values in B. (B) Mean response magnitude (determined in four fish, based on 64 switches at each position) for a switch occurring at the indicated positions along the fish at a distance of 3 mm from the skin. Note that the response was maximal for a dipole positioned at the tip of the Schnauzenorgan. NS, not significant.

is different from that at other body regions but vectors are also collimated. It is approximately 45° in contrast to almost 90° for the other body regions investigated. To affect the signal carrier at the Schnauzenorgan an object has to be placed right in front of the animal. The funnelling of the current by the geometry of the animal's body has been shown for *Gymnotus carapo* (Castelló et al., 2000) and *G. petersii* (this study). It might be interesting to compare our data to those of other fish species. For example, the model of Assad [see fig. 1 in (Assad et al., 1999)] indicates that in the well-studied wave-type species of *Eigenmannia* and *Apteronotus* the head does not seem to experience the strongest field intensities. Future experimental studies, including models of electric images at various body regions (Babineau et al., 2007; Rasnow and Bower, 1996) are needed to evaluate if these fish rely less on the information derived from the head electroreceptors than pulse-type electric fish.

Second, with respect to receptor density, both foveal regions are characterised by an extraordinarily high density of mormyromasts with the highest densities occurring at the tip of the Schnauzenorgan. Concerning the third characteristic of a fovea, central over-representation, no data were obtained in this study. However, other work (Bacelo and Grant, 2001; Bell, 1990; Bell et al., 1989) showed that the nasal region and the Schnauzenorgan are disproportionately highly represented in the electrosensory lateral line lobe (ELL), the first sensory station in the brain. Interestingly, this over-representation is specific for the mormyromast receptor organs, which are thought to be used primarily for active electrolocation and encode amplitude and phase distortions of the LEODs caused by objects. For the Schnauzenorgan and not for the nasal region, a specific central over-representation of phasic electroreceptor cells (B-cells) (Bacelo and Grant, 2001) exists, which again supports a functional separation of the two foveal regions.

Finally, the presence of a fovea, which is a small part of a receptive mosaic of highest resolution, requires a behavioural orientating of the fovea towards objects of interest in the environment. Such motor behaviours have indeed been found for the Schnauzenorgan, which is moved in a stereotyped, rhythmic manner during foraging. During exploratory and foraging behaviours, *Gnathonemus* can move the Schnauzenorgan with a high velocity of up to 800° s^{-1}. These regular movements are often associated with EOD frequencies of 60–80 Hz. Thus, *Gnathonemus* scans the direct surrounding of the Schnauzenorgan at a rate of up to 10°/EOD (M.H., unpublished). For these movements the importance of the pre-receptor effects is obvious: they stabilise the electric field at the Schnauzenorgan tip. Thus, the receptors on the Schnauzenorgan perceive a constant field in the absence of external stimuli, and stimulation is not altered by self-generated motions. In other weakly electric fishes such re-afferent sensory stimulation caused by body movements has been found, and in these animals they require additional central filter mechanisms to deal with this phenomenon.

All four of the above mentioned characteristics of a fovea are present for the Schnauzenorgan and at least three were found for the nasal region. Currently, we have no proof of specific orienting behaviours for the nasal region but it is tempting to speculate that the observed preferred angle at which the nasal region is held during foraging in *Gnathonemus* (Hollmann and von der Emde, 2007) could serve as a specialisation to position the nasal region at an optimal angle for active electrolocation of objects. When looking for food on the ground, *G. petersii* swims at a constant body axis angle of 18°±3.6° to the ground and simultaneously performs the above-mentioned rhythmic movements with its Schnauzenorgan. By swimming in this position, the sensory surface of the nasal region is held almost constant at an angle of 50°±5.8° relative to the ground (Hollmann and von der Emde, 2007). It thus points forward and slightly upward and might be in an optimal position to detect approaching objects such as obstacles or environmental landmarks.

During foraging, *Gnathonemus petersii* is searching for small prey objects, mostly insect larvae that live on the bottom of the stream, which constitute the major food source of *Gnathonemus*. In addition to detection and identification of close-by objects, the Schnauzenorgan can also be used for digging in the benthos to retrieve the food (G.v.d.E., personal observation). The nasal region, however, can be regarded as being optimised for the representation of electric images of objects in front of and at the sides of the animal's head, i.e. it is best suited for spatial active electrolocation. It is at the nasal region where the coherence of LEODs is maximal and the vectorial components are equal. This suggests that objects at any position between 0° (animal's front) and ±90° (animal's side) distort the local electric field in a similar way and therefore project similar electric images onto the nasal region. This will enable the fish to localise and possibly classify objects over a wide electrolocation angle around the head. During the usual foraging mode at the ground, the nasal region is held at a constant angle relative to the ground when the fish swims forward. While the Schnauzenorgan scans the ground with rhythmic sweeping movements, the nasal region is simultaneously used to monitor the space around the animal's head. When the fish approaches an obstacle, this object projects an electric image onto the nasal region and is thus detected and may be identified. The nasal region can also be used during catching of copepods suspended in the water. Because these prey items swim in the open water, they are usually not detected by the Schnauzenorgan unless they are very close. They will be more likely detected by the nasal region as the fish swims past them, causing a startle response and resulting in an orienting response of the Schnauzenorgan towards the prey, which is finally followed by ingestion of the prey.

Our data show that in *G. petersii* the LEOD and current vector trajectories are different at the trunk of the fish compared to the head, including the Schnauzenorgan. A similar finding was made for *Gymnotus carapo* where the phase changes of the EOD can be explained by the innervation of a complex, variable, and long electric organ and a non-synchronous generation of the EOD (Aguilera et al., 2001). In contrast to *Gymnotus*, this explanation does not apply to *G. petersii*, which have a synchronously activated electric organ that is present only in a short region of the tail. It seems more likely that the distortions seen in the trajectory of the current vectors are due to differences in skin resistance and capacitance in different body regions. Both components are highest in the nasal region and at the Schnauzenorgan (von der Emde and Schwarz, 2002). Owing to capacitive loading of the head region during the outward phase of current flow, the current flow in the y axis will be different from that in the z axis, causing a loop in the vector trajectory at the trunk (Fig. 2). The properties of the skin are very similar over the whole head region and hence the components building the LEOD are highly in phase.

In order to understand how electric images are displayed on the foveal electrosensory surface, we recorded electric images of cubes and spheres at the nasal region of *G. petersii*. Electric images of different types of objects could easily be distinguished from one another. One of the cues *G. petersii* might use to discriminate between differently shaped objects could be the slope of the electric image. In contrast to the electric images recorded (von der Emde et al., 1998) or modelled (Sicardi et al., 2000) at the trunk of the animal, the slope of the electric images of spheres was steeper than

that of cubes at the nasal region. The steepness of the slope is mainly due to the so-called edge effect (Sicardi et al., 2000). When the sensory surface, i.e. the projection plane for the electric images is flat, the projection of any object that faces this surface with a flat side is characterised by a plateau. At the end of the object the plateau stops abruptly, which leads to high slope values at the edges of the electric images. In contrast to the trunk, the foveal region at the front of the head is strongly curved. Therefore, no plateau can develop for cube-like objects, and the electric image is less steep because the drain of current through the edges of the object results in a smoother but widened voltage distribution. The opposite applies for images of spheres. Because the edge effect caused by a sphere is less strong, the resulting electric image is attenuated. It is smaller and its slope becomes steep because the LEOD amplitude is affected twice by the curvature of the sensory surface and by the curvature of the object (Fig. 13).

Another interesting difference with regard to the images that were measured (von der Emde et al., 1998) or modelled (Sicardi et al., 2000) at the trunk of the animal was the absence of an opposite surround or Mexican-hat effect. At the head of the animals this centre/surround organisation of electric images was not found. Instead of being bilaterally symmetrical, a modulation smaller than one, i.e. a drain of current, was found at the Schnauzenorgan (Fig. 10). This gives rise to the speculation that the Mexican-hat effect might not be essential for the animal to correctly determine the slope/amplitude ratio for distance discrimination. However, it remains possible that the Mexican-hat effect that occurs at the trunk is optimal for precise measurements of image slopes because it increases the contrast of the image, especially when considering relative motion between object and fish (Babineau et al., 2007).

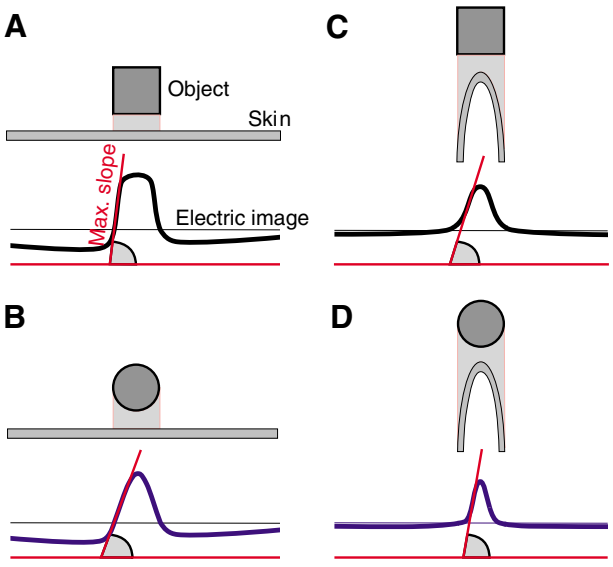

Fig. 13. Schematic illustrations of the ambiguity of the slope of electric images at different body regions. (A) A cube opposite a flat sensory surface. The distance between the object and the sensory surface is constant. The resulting electric image is bell-shaped and the slope is steep (depicted by the red line intersecting the horizontal line to indicate the angles). (B) A spherical object opposite a flat sensory surface. The edges of the object are farther away than the middle of the object. Therefore the slope of the electric image is less steep. (C) A cube opposite a curved sensory surface. The edges of the object are farther away than the middle of the object. Compared to the trunk the slope is less. (D) A spherical object facing a curved sensory surface. As the distance between the edges of the object and the sensory surface is greater than for the flat surface (B) the slope is steeper.

The initial experiments by von der Emde et al. (von der Emde et al., 1998) identified the ratio of the peak amplitude to the maximum rostral slope of the object image as the parameter most probably used by the electrosensory system to judge distance. These authors noted that caudal slope of the image was too variable to be a reliable index. In contrast, no distortions occur in the electric image projected on the head region, again pointing to the idea that this region is ideal for the faithful projection and analysis of electric images.

Given the asymmetry of the distribution of the electroreceptors and the pre-receptor mechanisms focussing the electric field at the foveal regions, it is not surprising that a central overrepresentation of the foveal areas in the ELL was recently found (K. Grant, J. Bacelo, J. Engelmann, M. Hollmann and G. von der Emde, manuscript submitted for publication). In experiments on the spatial representation of the sensory world at the different body regions it was found that the foveation is not linked to the size of receptive fields (H. Metzen, J. Engelmann, J. Bacelo, K. Grant and G. von der Emde, manuscript submitted for publication), i.e. receptive fields in the ELL are on average five times larger than those of the primary afferents but their size is not related with the location on the body surface. Similar findings were obtained in gymnotide fish where the head has the highest receptor density. As well, the head is centrally strongly represented (Carr, 1982) and receptive field sizes in the ELL are constant throughout the somatotopic map (Shumway, 1989). How these parameters influence the resolution of the electrosensory system has not yet been tested experimentally. It is to be expected that neurones receiving input from the foveal areas are likely to have a stronger overlap with neighbouring neurones, resulting in a better resolution of the electrosensory image at the population level (see Lewis and Maler, 2001). Based on the assumption that information contained in electric images is processed in a population code (Lewis and Maler, 2001; Assad et al., 1999), this should result in an increased spatial acuity at foveal regions. Although our behavioural data, using the strength of the novelty response as a measure, indicate that the fovea is associated with minimal thresholds for perceiving changes in the electrosensory scenery. In future experiments we hope to directly compare the spatial resolution for the different regions of the animals' body using the novelty response in conjunction with natural electric images.

Summarising our results, we have shown that pre-receptor mechanisms and morphological adaptations optimise the electric field for electrolocation. These mechanisms are of utter importance in the head regions, enabling the Schnauzenorgan to be used as a mobile sensor. In fact, the funnelling effect allows the Schnauzenorgan to be used as an electrical searchlight as it will 'illuminate' objects under inspection. With respect to electric images we, for the first time, measured these for cubic and spherical objects at the head region. Our data substantially differ from published work that showed that spheres had shallower slopes in their electric image then cubes (Sicardi et al., 2000). This is important since these slopes are used by the fish to determine distance to objects (Schwarz and von der Emde, 1998). In Fig. 13 we present a schematic explaining why this difference exists.

Currently we cannot determine if fish can use either slope measure (trunk and/or head) to determine distance, or if a division of labour is present regarding the information extraction from electric images. Our behavioural work, however, suggests that the Schnauzenorgan and to a lesser extend the head region are, as a result of the pre-receptor mechanisms and the high receptor densities, ideal for

detailed analyses of electric images, whereas the trunk probably has a weaker acuity.

LIST OF ABBREVIATIONS

ELL	electrosensory lateral line lobe
EOD	electric organ discharge
HEOD	head to tail electric organ discharge
LdEOD	local distorted electric organ discharge
LEOD	local electric organ discharge

This work was supported by a Marie Curie Fellowship from the European Commission to J.E. (QLK6-CT-2002-5172) and a grant from the German Science Foundation (DFG, EN 826/1-1). R.P. is supported by a fellowship from the Friedrich-Ebert-Foundation. We thank two anonymous reviewers and Dipl. Inf. Tobias Kunze for critical comments on the manuscript, and Dr A. Mickenhagen for technical support.

REFERENCES

Aguilera, P. A. and Caputi, A. A. (2003). Electroreception in *G carapo*: detection of changes in waveform of the electrosensory signals. *J. Exp. Biol.* **206**, 989-998.
Aguilera, P. A., Castelló, M. E. and Caputi, A. A. (2001). Electroreception in *Gymnotus carapo*: differences between self-generated and conspecific-generated signal carriers. *J. Exp. Biol.* **204**, 185-198.
Assad, C., Rasnow, B. and Stoddard, P. K. (1999). Electric organ discharges and electric images during electrolocation. *J. Exp. Biol.* **202**, 1185-1193.
Azzopardi, P. and Cowey, A. (1993). Preferential representation of the fovea in the primary visual cortex. *Nature* **361**, 719-721.
Azzopardi, P. and Cowey, A. (1996). The overrepresentation of the fovea and adjacent retina in the striate cortex and dorsal lateral geniculate nucleus of the macaque monkey. *Neuroscience* **72**, 627-639.
Babineau, D., Lewis, J. E. and Longtin, A. (2007). Spatial acuity and prey detection in weakly electric fish. *PLoS Comput. Biol.* **3**, e38.
Bacelo, J. and Grant, K. (2001). Electrosensory and trigeminal innervation of the Schnauzenorgan in *Gnathonemus petersii*. In *6th International Congress of Neuroethology*, pp. 225. Bonn/Germany.
Bastian, J. (1995). Pyramidal-cell plasticity in weakly electric fish: a mechanism for attenuating responses to reafferent electrosensory inputs. *J. Comp. Physiol. A* **176**, 63-73.
Bell, C. C. (1990). Mormyromast electroreceptor organs and their afferent fibers in mormyrid fish. II. Intra-axonal recordings show initial stages of central processing. *J. Neurophysiol.* **63**, 303-318.
Bell, C. C., Zakon, H. and Finger, T. E. (1989). Mormyromast electroreceptor organs and their afferent fibers in mormyrid fish. I. Morphology. *J. Comp. Neurol.* **286**, 391-407.
Budelli, R., Caputi, A. A., Gomez, L., Rother, D. and Grant, K. (2002). The electric image in *Gnathonemus petersii*. *J. Physiol. Paris* **96**, 421-429.
Caputi, A. A. (2004). Contributions of electric fish to the understanding of sensory processing by reafferent systems. *J. Physiol. Paris* **98**, 81-97.
Caputi, A. and Budelli, R. (1995). The electric image in weakly electric fish. I. A data-based model of waveform generation in *Gymnotus carapo*. *J. Comput. Neurosci.* **2**, 131-147.
Caputi, A. A. and Budelli, R. (2006). Peripheral electrosensory imaging by weakly electric fish. *J. Comp. Physiol. A* **192**, 587-600.
Caputi, A. A., Budelli, R., Grant, K. and Bell, C. C. (1998). The electric image in weakly electric fish: physical images of resistive objects in Gnathonemus petersii. *J. Exp. Biol.* **201**, 2115-2128.
Caputi, A. A., Castello, M. E., Aguilera, P. and Trujillo-Cenoz, O. (2002). Electrolocation and electrocommunication in pulse gymnotids: signal carriers, pre-receptor mechanisms and the electrosensory mosaic. *J. Physiol. Paris* **96**, 493-505.
Caputi, A. A., Aguilera, P. A. and Castello, M. E. (2003). Probability and amplitude of novelty responses as a function of the change in contrast of the reafferent image in *G. carapo*. *J. Exp. Biol.* **206**, 999-1010.
Carr, C. E., Maler L. and Sas, E. (1982). Peripheral organization and central projections of the electrosensory nerves in gymnotiform fish. *J. Comp. Neurol.* **211**, 139-153.
Castelló, M. E., Aguilera, P. A., Trujillo-Cenoz, O. and Caputi, A. A. (2000). Electroreception in *Gymnotus carapo*: pre-receptional mechanisms and distribution of electroreceptor types. *J. Exp. Biol.* **203**, 3279-3287.
Catania, K. C. and Remple, F. E. (2004). Tactile foveation in the star-nosed mole. *Brain Behav. Evol.* **63**, 1-12.
Ciali, S., Gordon, J. and Moller, P. (1997). Spectral sensitivity of the weakly discharging electric fish *Gnathonemus petersii* using its electric organ discharges as the response measure. *J. Fish Biol.* **50**, 1074-1087.
Coombs, S., New, J. G. and Nelson, M. (2002). Information-processing demands in electrosensory and mechanosensory lateral line systems. *J. Physiol. Paris* **96**, 341-354.
Engelmann, J., Bacelo, J., van den Burg, E. and Grant, K. (2006). Sensory and motor effects of etomidate anesthesia. *J. Neurophysiol.* **95**, 1231-1243.
Gómez, L., Budelli, R., Grant, K. and Caputi, A. A. (2004). Pre-receptor profile of sensory images and primary afferent neuronal representation in the mormyrid electrosensory system. *J. Exp. Biol.* **207**, 2443-2453.
Hall, C., Bell, C. and Zelick, R. (1995). Behavioral evidence of a latency code for stimulus intensity in mormyrid electric fish. *J. Comp. Physiol. A* **177**, 29-39.
Harder, W. (1968). Die Beziehungen zwischen Elektrorezeptoren, elektrischen Organen, Seitenlinienorganen und Nervensystem bei den Mormyridae (Teleostei, Pisces). *Z. Vergl. Physiol.* **59**, 272-318.
Harder, W., Schief, A. and Uhlemann, H. (1967). Zur Empfindlichkeit des schwachelektrischen Fisches *Gnathonemus petersii* (Mormyriformes; Teleostei) gegenüber elektrischen Feldern. *Z. Vergl. Physiol.* **54**, 89-108.
Hollmann, M. and von der Emde, G. (2004). Electroreceptor organs in two 'electrical foveae' of the weakly electric fish, *Gnathonemus petersii*. In *Proceedings of the 7th International Congress of Neuroethology*. Nyborg, Denmark.
Hollmann, M. and von der Emde, G. (2007). Electrofoveal regions on the skin of a weakly electric fish. In *8th International Congress of Neuroethology*. Vancouver, Canada.
Lewis, J. E. and Maler, L. (2001). Neuronal population codes and the perception of object distance in weakly electric fish. *J. Neurosci.* **21**, 2842-2850.
Lissmann, H. W. and Machin, K. E. (1958). The mechanism of object location in *Gymnarchus niloticus* and similar fish. *J. Exp. Biol.* **35**, 451-486.
Malmstrom, T. and Kroger, R. H. (2006). Pupil shapes and lens optics in the eyes of terrestrial vertebrates. *J. Exp. Biol.* **209**, 18-25.
Migliaro, A., Caputi, A. A. and Budelli, R. (2005). Theoretical analysis of pre-receptor image conditioning in weakly electric fish. *PLoS Comp. Biol.* **1**, 123-131.
Post, N. and von der Emde, G. (1999). The "novelty response" in an electric fish: response properties and habituation. *Physiol. Behav.* **68**, 115-128.
Rasnow, B. (1996). The effects of simple objects on the electric field of *Apteronotus*. *J. Comp. Physiol. A* **178**, 397-411.
Rasnow, B. and Bower, J. M. (1996). The electric organ discharges of the Gymnotiform fishes. I. *Apteronotus leptorhynchus*. *J. Comp. Physiol. A* **178**, 383-396.
Schwarz, S. (1997). Entfernungsmessung mit Hilfe der Elektroortung beim schwach-elektrischen Fisch *Gnathonemus petersii*. Diploma thesis, Zoological Institute, University of Bonn, Germany.
Schwarz, S. (2000). *Gnathonemus petersii*: three-dimensional object shape detection and the geometry of the self-produced electric field. PhD Thesis, Zoological Institute, University of Bonn, Germany.
Schwarz, S. and von der Emde, G. (1998). Distance discrimination in the electric fish *Gnathonemus petersii*. In *New Neuroethology on the Move: Proceedings of the 26th Göttingen Neurobiology Conference 1998*. Vol. I (ed. N. Elsner and R. Wehner), p. 51. Stuttgart, New York: Thieme.
Schwarz, S. and von der Emde, G. (2001). Distance discrimination during active electrolocation in the weakly electric fish *Gnathonemus petersii*. *J. Comp. Physiol. A* **186**, 1185-1197.
Shumway, C. A. (1989). Multiple electrosensory maps in the medulla of weakly electric gymnotiform fish. I. Physiological differences. *J. Neurosci.* **9**, 4388-4399.
Sicardi, E. A., Caputi, A. A. and Budelli, R. (2000). Physical basis of distance discrimination in weakly electric fish. *Physica A* **283**, 86-93.
Szabo, T. and Fessard, A. (1965). Le fonctionnement des électrorécepteurs étudié chez les Mormyres. *J. Physiol. Paris* **57**, 343-360.
von der Emde, G. (2006). Non-visual environmental imaging and object detection through active electrolocation in weakly electric fish. *J. Comp. Physiol. A* **192**, 601-612.
von der Emde, G. and Schwarz, S. (2002). Imaging of objects through active electrolocation in *Gnathonemus petersii*. *J. Physiol. Paris* **96**, 431-444.
von der Emde, G., Schwarz, S., Gomez, L., Budelli, R. and Grant, K. (1998). Electric fish measure distance in the dark. *Nature* **395**, 890-894.
Wagner, H. J. (2007). Bipolar cells in the "grouped retina" of the elephantnose fish (*Gnathonemus petersii*). *Vis. Neurosci.* **24**, 355-362.